UC Davis
Research Reports

Title
Deep Learning–based Eco-driving System for Battery Electric Vehicles

Permalink
https://escholarship.org/uc/item/9fz140zt

Authors
Wu, Guoyuan
Ye, Fei
Hao, Peng
et al.

Publication Date
2019-05-01

DOI
10.7922/G2NP22N6

Data Availability
The data associated with this publication are available at: https://doi.org/10.6086/D1FW9G

eScholarship.org Powered by the California Digital Library
University of California

Deep Learning–based Eco-driving System for Battery Electric Vehicles

May 2019

A Research Report from the National Center for Sustainable Transportation

Guoyuan Wu, University of California, Riverside
Fei Ye, University of California, Riverside
Peng Hao, University of California, Riverside
Danial Esaid, University of California, Riverside
Kanok Boriboonsomsin, University of California, Riverside
Matthew J. Barth, University of California, Riverside

National Center for Sustainable Transportation
UCR College of Engineering- Center for Environmental Research & Technology

TECHNICAL REPORT DOCUMENTATION PAGE

1. Report No. NCST-UCR-RR-19-03	**2. Government Accession No.** N/A	**3. Recipient's Catalog No.** N/A
4. Title and Subtitle Deep Learning–based Eco-driving System for Battery Electric Vehicles		**5. Report Date** May 2019 **6. Performing Organization Code** N/A
7. Author(s) Guoyuan Wu, PhD https://orcid.org/0000-0001-6707-6366; Fei Ye; Peng Hao, PhD https://orcid.org/0000-0001-5864-7358; Danial Esaid; Kanok Boriboonsomsin, PhD https://orcid.org/0000-0003-2558-5343; Matthew J. Barth, PhD https://orcid.org/0000-0002-4735-5859		**8. Performing Organization Report No.** N/A
9. Performing Organization Name and Address University of California, Riverside Bourns College of Engineering – Center for Environmental Research & Technology 1084 Columbia Avenue Riverside, CA 92507		**10. Work Unit No.** N/A **11. Contract or Grant No.** USDOT Grant 69A3551747114
12. Sponsoring Agency Name and Address U.S. Department of Transportation Office of the Assistant Secretary for Research and Technology 1200 New Jersey Avenue, SE, Washington, DC 20590		**13. Type of Report and Period Covered** Final Report (July 2017 – May 2019) **14. Sponsoring Agency Code** USDOT OST-R
15. Supplementary Notes DOI: 10.7922/G2NP22N6 Dataset DOI: https://doi.org/10.6086/D1FW9G		

16. Abstract

Eco-driving strategies based on connected and automated vehicles (CAV) technology, such as Eco-Approach and Departure (EAD), have attracted significant worldwide interest due to their potential to save energy and reduce tail-pipe emissions. In this project, the research team developed and tested a deep learning–based trajectory-planning algorithm (DLTPA) for EAD. The DLTPA has two processes: offline (training) and online (implementation), and it is composed of two major modules: 1) a solution feasibility checker that identifies whether there is a feasible trajectory subject to all the system constraints, e.g., maximum acceleration or deceleration; and 2) a regressor to predict the speed of the next time-step. Preliminary simulation with microscopic traffic modeling software PTV VISSIM showed that the proposed DLTPA can achieve the optimal solution in terms of energy savings and a greater balance of energy savings vs. computational efforts when compared to the baseline scenarios where no EAD is implemented and the optimal solution (in terms of energy savings) is provided by a graph-based trajectory planning algorithm.

17. Key Words Eco-driving, deep-learning, energy and emissions, VISSIM	**18. Distribution Statement** No restrictions.

19. Security Classif. (of this report) Unclassified	**20. Security Classif. (of this page)** Unclassified	**21. No. of Pages** 37	**22. Price** N/A

NCST

About the National Center for Sustainable Transportation

The National Center for Sustainable Transportation is a consortium of leading universities committed to advancing an environmentally sustainable transportation system through cutting-edge research, direct policy engagement, and education of our future leaders. Consortium members include: University of California, Davis; University of California, Riverside; University of Southern California; California State University, Long Beach; Georgia Institute of Technology; and University of Vermont. More information can be found at: ncst.ucdavis.edu.

U.S. Department of Transportation (USDOT) Disclaimer

The contents of this report reflect the views of the authors, who are responsible for the facts and the accuracy of the information presented herein. This document is disseminated in the interest of information exchange. The report is funded, partially or entirely, by a grant from the U.S. Department of Transportation's University Transportation Centers Program. However, the U.S. Government assumes no liability for the contents or use thereof.

Acknowledgments

This study was funded by a grant from the National Center for Sustainable Transportation (NCST), supported by USDOT through the University Transportation Centers program. The authors would like to thank the NCST and USDOT for their support of university-based research in transportation, and especially for the funding provided in support of this project. The authors would like to also thank Dr. Xuewei Qi for his constructive comments over the project and Mr. Yingqiao Jiang for help on data collection.

Deep Learning–based Eco-driving System for Battery Electric Vehicles

A National Center for Sustainable Transportation Research Report

May 2019

Guoyuan Wu, Center for Environmental Research & Technology, University of California, Riverside

Fei Ye, Center for Environmental Research & Technology, University of California, Riverside

Peng Hao, Center for Environmental Research & Technology, University of California, Riverside

Danial Esaid, Center for Environmental Research & Technology, University of California, Riverside

Kanok Boriboonsomsin, Center for Environmental Research & Technology, University of California, Riverside

Matthew J. Barth, Center for Environmental Research & Technology, University of California, Riverside

NCST

[page intentionally left blank]

TABLE OF CONTENTS

List of Tables

List of Figures

Deep Learning–based Eco-driving System for Battery Electric Vehicles

EXECUTIVE SUMMARY

The uninterrupted growth in transportation activities, for both people and goods movement, has been exerting significant pressure on our socio-economics and environment. However, emerging technologies such as connected and automated vehicles (CAVs), transportation electrification, and edge computing have been stimulating increased efforts by engineers, researchers, and policymakers to tackle transportation-related problems, including those focused on energy and the environment. The eco-driving strategies based on CAV technology particularly have attracted significant interest from all over the world due to its potential to save energy and reduce tail-pipe emissions. Among all CAV based eco-driving strategies, the Eco-Approach and Departure (EAD) application at Signalized Intersections has shown the most significant promise. In this system, an equipped vehicle can take advantage of the signal phase and timing (SPaT) and geometric intersection description (GID) information from the upcoming signalized intersection and calculate the optimal speed to pass on a green light or to decelerate to a stop in the most eco-friendly manner. Speed recommendations may be provided to the driver using a driver-vehicle-interface (DVI) or to the vehicle systems that support automated longitudinal control capabilities.

In this project, the research team conducted a thorough literature review of EAD algorithms, and identified a major research gaps in the following areas: (1) the balance between system optimality and computational efficiency; (2) designated algorithms for electric vehicles (e.g., consideration of regenerative braking); and (3) taking into account downstream traffic information (e.g., prediction of preceding vehicle's state). To address these gaps, the research team proposed a deep learning–based trajectory-planning algorithm (DLTPA) for EAD application, which can be considered as an approximation of a global optimal algorithm (called a graph-based trajectory planning algorithm or GTPA) that the research team previously developed. The proposed DLTPA has two processes: offline (training) and online (implementation), and it is composed of two major modules: 1) a solution feasibility checker that identifies whether there is a feasible trajectory subject to all the system constraints, e.g., maximum acceleration or deceleration; and 2) a regressor to predict the speed of the next time step.

Preliminary simulation study in microscopic traffic modeling software PTV VISSIM showed that the proposed DLTPA can achieve a great balance of energy savings vs. computational efforts when compared to the baseline scenario where no EAD was implemented and the optimal solution (in terms of energy savings) was provided by GTPA.

Introduction

The uninterrupted growth in transportation activities, for both people and goods movement, has exerted significant pressure on our socio-economics and environment. The transportation sector in the United States consumed approximated 27.5 quadrillion BTUs (British thermal unit) of energy in 2016, 92.2% percent of which came from petroleum [*1*]. In addition, the latest annual report by the U.S. Environmental Protection Agency (USEPA) estimated that surface transportation modes (such as passenger cars, trucks, buses, and motorcycles) contributed 1,556 MMT CO_2eq to greenhouse gas (GHG) emissions in 2016, accounting for 28.5% of nationwide GHG emissions [*2*]. According to the same report, transportation just slightly surpassed the electric power industry (28.4%) and became the largest source of GHG across all U.S. economic sectors in 2016.

On the other hand, emerging technologies such as connected vehicles (CV), transportation electrification, and edge computing have stimulated increased efforts from engineers, researchers and policymakers to tackle transportation-related energy and environmental problems. Good examples include the Applications for the Environment: Real-Time Information Synthesis (AERIS) Program initiated by the U.S. Department of Transportation [*3*], and the eCoMove project funded by the European Commission [*4*]. A variety of environmentally-friendly CV applications, in particular those related to eco-driving strategies, have been proposed, developed, and validated [*5*]. Among all environmentally-friendly eco-driving strategies, the Eco-Approach and Departure (EAD) at Signalized Intersections application has shown significant promise [*6*–*10*]. In this system, a vehicle can take advantage of the signal phase and timing (SPaT) and geometric intersection description (GID) information from the upcoming signalized intersection and calculate the optimal speed to pass on a green light or to decelerate to a stop in the most eco-friendly manner. Speed recommendations may be provided to the driver using a driver-vehicle-interface (DVI) or to the vehicle systems that support automated longitudinal control capabilities.

Due to the benefits of EAD-like eco-driving algorithms, numerous studies have focused on their development and testing [*11*–*20*]. However, many of these algorithms are not flexible enough to effectively handle customized powertrain characteristics, interaction with other traffic, road grade, and travel through multiple intersections [*33*]. This project aims to address some of these gaps, and the uniqueness of this research includes:

- *Customized electric powertrain*. Based on real world data, an electric vehicle (EV) energy consumption model is developed and integrated into a new eco-driving algorithm and the regenerative braking effect is taken into account.
- Prediction of downstream vehicle's trajectory. Machine learning technique is applied to a snippet of a vehicle's downstream trajectory (which may be obtained from an on-board sensor, such as radar) to predict its movement (e.g., stopping, acceleration, cruising). This information may help the vehicle better plan its trajectory for saving energy.

- Deep learning–based EAD algorithm. This algorithm can achieve a balance between solution optimality and computational efficiency.

Literature Review

In this section, we first review previous research on Eco-Approach and Departure (EAD) applications and then give a brief introduction on the powertrain model used for fuel/energy consumption estimation in this study.

The State-of-the-Art on Eco-Approach and Departure

In the past decade, a variety of studies have been conducted on EAD, especially from the perspective of an isolated intersection. *Mandava et al*. [*11*] proposed a piecewise linear-trigonometric function–based vehicle trajectory planning algorithm for eco-driving along an urban arterial road. The algorithm was extensively evaluated and validated in simulations [*21*] and field testing [*22*], in the form of an advanced driver assistance system [*23*] and partially automated control [*24*]. It showed excellent real-time performance and substantial benefits in reducing fuel consumption and tailpipe emissions. However, significant efforts may be necessary to modify the algorithm to adapt it to customized powertrain models and rolling terrain. Based on the VT-Micro[1] model, *Rakha* and *Kamalanathsharma* [*13*] developed a constant deceleration based eco-driving strategy to avoid full stops at signals. They later improved upon this, using multi-stage dynamic programming and recursive path-finding principles, as well as evaluation with an agent-based model [*25*]. *Asadi* and *Vahidi* [*14*] proposed a two-step predictive cruise control concept, aiming to reduce fuel use and trip time by using traffic signal status information. The first step is to determine the target speed based on an available green window, and the second step is to perform the optimal tracking of the target speed. *Katsaros et al.* [*15*] developed a Green Light Optimized Speed Advisory (GLOSA) system designed to minimize average fuel consumption and average stop delay at a traffic signal. By taking into account the queue discharging process, *Chen et al.* [*16*] developed an eco-driving algorithm for a vehicle approaching and leaving a signalized intersection to minimize a linear combination of emissions and travel time, without taking into account roadway grade information. *Jin et al.* [*17*] formulated the power-based optimal longitudinal connected eco-driving problem into a 0-1 Binary Mixed Integer Linear Programming (MILP), which is applicable to signalized intersections, non-signalized intersections, and freeways. The approach can take into account road grade effects and powertrain dynamics, but has relatively low computational efficiency. *Li et al.* [*18*] used the Legendre Pseudo-Spectral method and knotting technique to overcome the discrete gear ratio issue in the optimal control for eco-driving at signalized intersections. *Huang* and *Peng* [*19*] adopted a simplified powertrain model and applied the Sequential Convex Optimization approach to optimize vehicle speed trajectory at signalized intersections, which aimed to keep a balance between the optimality and real-time performance.

[1] A microscopic vehicle energy/emission model developed by Virginia Polytechnic Institute and State University

When considering the application of an Eco-Approach and Departure system in a more realistic environment, many studies took a "reactive" approach to cope with the disturbance from the downstream traffic (e.g., switching to the car-following mode control if the subject vehicle was too close to its predecessor) or assumed traffic signals were running in a fixed-time mode [*20, 26*, *27*]. To address these issues, some researchers specifically focused on tackling the queuing effects for Eco-Approach and Departure at Signalized Intersections (EADSI) by applying the shockwave theory [*28*] or data-driven techniques [*29*] to predict the queue length or, in essence, the trajectory of the subject vehicle's predecessor. Other approaches were dedicated to dealing with uncertainties in traffic signal operation such as countdown information by improving the prediction of SPaT [*30*] or developing more robust eco-driving strategies [*31*, *32*].

Estimation of Electric Vehicle Energy Consumption

Recently, a good deal of effort has been devoted to developing estimation models for energy consumption in electric vehicles [*34–42*]. Several studies established EV energy consumption estimation models at different granularity for the purpose of eco-routing applications [*42*], assessment of different aggregation level influence on energy consumption [*36*], and eco-driving on urban arterial roads [*35*].

From the perspective of modeling methodology, the knowledge-driven ("white-box") approach either considers the vehicle as a point-mass by applying Newton's Laws (analytical model) or builds up a detailed physical process for each module in an electric vehicle [*34*, *38*, *40*]. This approach has the advantage of providing a direct link between vehicle or power train dynamics and the variables affecting energy consumption. However, the knowledge-driven models may be too generic without differentiating the powertrain type or overly complex in real-time implementation. For example, Wu et al. [*40*] used real-world measurements and established an instantaneous EV energy consumption model directly derived from the vehicle dynamics. All the parameters in their model are reduced to predetermined constants. In contrast, the data-driven ("black-box") approach applies statistical techniques [*35*, *39*] or machine learning algorithms [*37*] to the dataset collected from a vehicle test bed or real-world driving. This approach may result in very accurate estimation results based on a customized dataset or a specific scenario. However, the applicability to another situation is questionable. In addition, the physical meanings of selected variables and interpretation of such models are not justifiable. Yao et al. [*39*] proposed a purely statistical model in which variables include a complete list of combinations of speed and acceleration up to the third order. The meaning of some variables is vague. Further, the results are validated only with data collected in an ideal environment without considering road grade effects. Table 1 lists some related work by other researchers on the EV energy consumption estimation.

Table 1. Summary of studies on EV energy consumption estimation.

Authors	Impact Factors	Energy Estimation Model	Granularity
Yang et al. [34]	speed, acceleration, road grade	Physical/ analytical model	Instantaneous
Zhang et al. [35]	speed, acceleration, state of charge	Polynomial regression	Instantaneous
Baouche et al. [36]	average speed	VEHLIB[2] consumption model	Trip-based
Alvarex et al. [37]	statistic values of speed, acceleration and jerk	Artificial neural network	Instantaneous
Chang N. and Hong J. [38]	speed, acceleration, road grade, cargo weight	Physical/ analytical model	Instantaneous
Yao et al. [39]	speed, acceleration, Vehicle Specific Power (VSP)	Polynomial regression	Instantaneous
Wu et al. [40]	speed, acceleration, road grade	Physical/ analytical model	Instantaneous
Felipe et al. [42]	speed, acceleration, jerk and road grade	Artificial neural network	Trip-based

Vehicle Movement Prediction

Accurate and reliable prediction of vehicle speed trajectory is an important component in many Intelligent Transportation Systems (ITS) applications, particularly for safety and environmental related applications. Making such predictions is a challenging task, as the vehicle speed trajectory may be affected by various dynamic factors, e.g., signal status, maneuvers of surrounding vehicles, and perhaps interruption from pedestrians. In the literature, various approaches for vehicle speed prediction have been investigated and evaluated [*43–51*]. In general, the existing vehicle speed prediction strategies can be categorized into two major classes: model-based approaches and data-driven approaches. The model-based approaches predict the vehicle speed trajectory based on pre-defined model structures such as Constant Speed Model, Constant Acceleration Model, Constant Yaw Rate and Acceleration Model [*43*].

[2] A hybrid vehicle simulation tool: https://www.eco7.ifsttar.fr/en/the-institute/ame2/laboratories/eco7-english/vehlib/

However, the underlying dynamics of human cognition, decision-making, and execution of drivers and vehicle systems are extremely complex and these simplified models may not be applicable [*44*]. On the other hand, data-driven approaches have recently been well investigated since they show more flexibility and applicability in representing system dynamics. Good examples of effective data-driven approaches for vehicle speed trajectory prediction include Non-Parametric Regression, Gaussian Mixture Regression and Artificial Neural Networks [*45*– *48*]. In a report by Houenou et al. [*46*], the defined maneuver recognition algorithm selected the best vehicle trajectory that would minimize a cost function by comparing the current maneuver to the pre-defined trajectory set on the highways. Considering the requirement for a large sample of vehicle trajectories and the complexity of maneuver recognition in urban areas, applying this algorithm real-world urban traffic is challenging. Gaussian Mixture Regression is another promising parametric method to approximate or predict vehicle trajectories by calculating a conditional probability density function that consists of a weighted linear combination of Gaussian component densities [*47*]. Artificial Neural Networks have been proven to be an effective method for accurately forecasting vehicle speed and position, due to their strong capability of capturing complex and nonlinear dynamics [*48*–*50*]. A comparative study of major parametric and non-parametric approaches for vehicle speed prediction on highways indicates that Artificial Neural Networks outperform all the other methods in terms of both predictive accuracy and applicability [*48*]. Some approaches (i.e., TrackT [*51*] and TMicroscope [*52*]) have been proposed to enhance tracking of RFID systems to retrieve trajectory information. These approaches could provide real time trajectory information with high accuracy and be combined with advanced predictors to improve the overall performance.

Deep Learning Approach and its Applications in Transportation

This section briefly reviews some recent publications on the application of deep-learning techniques to the transportation area.

Increasing transportation efficiency reliably and at a low cost becomes challenging as transportation infrastructure becomes more complex. Deterministic logic is often impractical because of the complexity of the challenges in modern transportation networks. Deep learning shows promise for solving transportation problems because of its ability to learn non-linear functions. Studies have shown that transportation modes can be predicted using Long Short Term Memory and Convolutional Neural Networks [*53*], [*54*]. Further studies have shown that traffic flow can be accurately predicted with deep learning [*55*], [*56*]. Deep learning also has applications to mitigating calibration challenges. One study used reinforcement learning to achieve adaptive ramp metering without calibration [*57*]. Moreover, deep learning can be used to predict vehicle speeds. Network wide traffic speed predictions had a high accuracy when images were used as training data [*58*]. Lastly, deep learning shows promise for enabling autonomous vehicles. Results from empirical evaluations showed how deep learning can be used to perform lane and vehicle detection at speeds required for real world scenarios [*59*].

A Hybrid Model for Electric Vehicle Energy Consumption

Data Acquisition and Processing

We developed our models for energy consumption rate estimation based on driving data collected from a test electric vehicle (2013 NISSAN LEAF) in real world traffic.

Data Acquisition

The field data were collected during two periods: 1) March–July 2013; and 2) July 2018. The test EV was equipped with two major data acquisition systems: the CONSULT III plus kit and GPS data logger (see Figure 1). These were used to access vehicle activities (e.g., instantaneous speed), energy related parameters (e.g., battery current and voltage), and real-time location information (i.e., latitude, longitude).

Figure 1. Data collection equipment: (*left*) CONSULT III plus kit to collect test vehicle's energy consumption and other vehicle activities data; (*right*) GPS data logger.

More specifically, the CONSULT III plus kit, which is designated for professional diagnostics of all NISSAN models (including NISSAN LEAF), can retrieve high resolution (up to 100 Hz) data from the vehicle's CAN bus, such as speed, current and voltage for each cell, A/C power, accessory power, and state of charge. On the other hand, the GPS data logger can report the latitude and longitude of the test EV in real-time. Such information can be synchronized with existing geographic information system (GIS) to acquire the network-wide index and grade information of the road link on which the vehicle is traveling.

We selected four typical routes near Riverside, California (USA) for real-world data collection: 1) SR 91-Magnolia loop; 2) Riverside Plaza-Towngate loop; 3) Columbia-Alessandro loop; and 4) Palmyrita Avenue close to CE-CERT. Figure 2 presents the SR 91-Magnolia loop which covers a major freeway (SR 91) and arterial road (Magnolia Ave.), and a variety of traffic conditions and

road grades. In total, more than 100 hours of vehicle driving data under real-world conditions were collected.

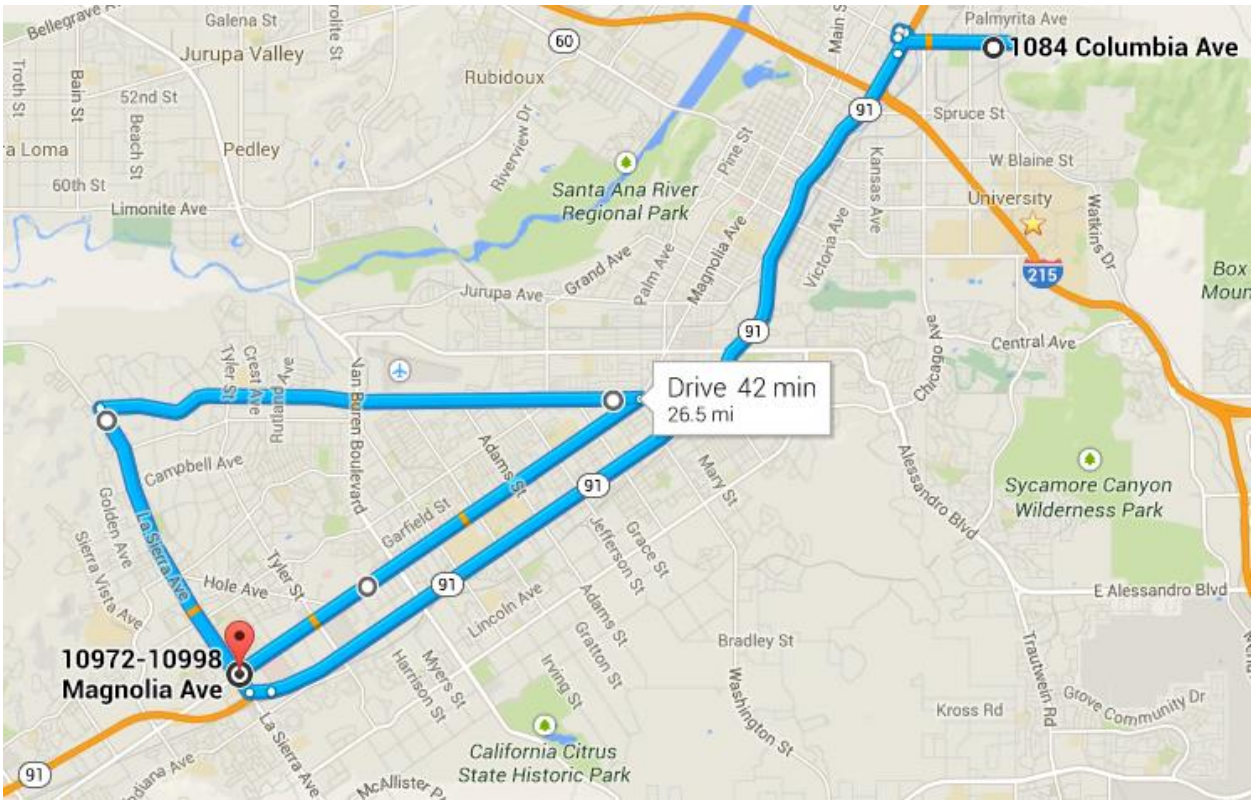

Figure 2. One of the field test loops consisting of SR-91 and Magnolia Ave., Riverside, California.

Data Processing

Before the application of the aforementioned field test data for model development, we first combined the dataset from the CONSULT III plus kit with that from the GPS data logger. This data fusion consists of two steps:

1) *Frequency realignment*. The frequency of raw GPS data was realigned into a 1-Hz signal, which is consistent with the data resolution from the CONSULT III plus kit and suitable for energy consumption estimation; and
2) *Trip start time synchronization*. Unlike the GPS data logger, the CONSULT III plus kit uses a relative time stamp (i.e., each run always starts from time "0") instead of a global time clock (i.e., Coordinated Universal Time). To synchronize these two datasets, we applied a cross-correlation technique on vehicle speed that was common to both data sources.

Modeling Approach

Power Flows at the Battery Terminal

The energy consumption of the electric vehicle considered in this study is specified as an integration of output power of the vehicle at the battery terminal. The equations for electric power for propulsion and regenerative braking at the battery terminal are as follows.

$$P_{b-out} = v(mg(fcos\alpha + sin\alpha) + 0.5\rho C_D A_f v^2 + m\delta dv/dt)/\eta_t\eta_m \quad (1)$$

$$P_{b-in} = kv\eta_t\eta_m(mg(fcos\alpha + sin\alpha) + 0.5\rho C_D A_f v^2 + m\delta dv/dt) \quad (2)$$

Here, η_t stands for the transmission efficiency and η_m represents motor drive efficiency. These two parameters are commonly approximated by a constant value. m is the EV's mass; f is the rolling resistance coefficient; g is the gravitational constant; ρ is the air density (kg/m^3); $C_D$is the aerodynamic drag coefficient; $A_f$is the EV's frontal area; δ is the coefficient related to the EV's mass; v is the vehicle's speed (m/s); α is the road grade (rad); k $(0 < k < 1)$ is the regenerative braking factor, which indicates the percentage of the total braking energy that can be recovered by the electric motor. The regenerative braking factor is actually a complex and time-varying coefficient which will be discussed in detail in a later section.

Thus, the total power flows at the battery terminal can be defined as:

$$P_{total} = P_{b-out} + P_{b-in} \quad (3)$$

In the real-world test data, the accessory power and A/C power were also measured, which turned out to be non-trivial and was therefore taken into account in the power estimation for the battery terminal.

Regenerative Braking Factor

Regenerative braking power is one of the most distinct features of electric vehicles and plays an important role in improving drivetrain efficiency. Compared to conventional internal combustion engine (ICE) vehicles, electric vehicles with regenerative braking have an advantage in energy efficiency, especially under stop-and-go driving scenarios. As mentioned in the above section, the regenerative braking factor, k, indicates the percentage of braking energy recovered back to charge the battery pack, implying the vehicle's recharging efficiency. The value of k is between 0 and 1 (in practice, k cannot reach 1 due to energy lost from battery internal resistance and cable resistance). Due to the complexity and time varying character of the regenerative braking factor k, it is essential to identify the factors that affect k in order to model electric vehicles' regenerative braking energy. According to a literature review, two major approaches have been used to model regenerative braking effects: a piecewise linear function of the vehicle's speed and a fuzzy logic model considering acceleration, jerk, and road grade as input variables (Figure 3). The first approach was derived based on the assumption that the regenerative braking factor can be represented by braking force, which is supposed to be linearly related to the vehicle's speed (see Eq. (4) in [39]). Please note that the equation is an approximation within a certain speed range (between 0 and 38 m/s). The second approach

considers a more complex regenerative braking process with the measurement data available for many factors (e.g., speed, acceleration, road grade) as shown in Figure 3.

$$k = \begin{cases} 0.5 \times v/5 & 0 \leq v < 5m/s \\ 0.5 + 0.3 \times (v-5)/20 & v \geq 5m/s \end{cases} \quad (4)$$

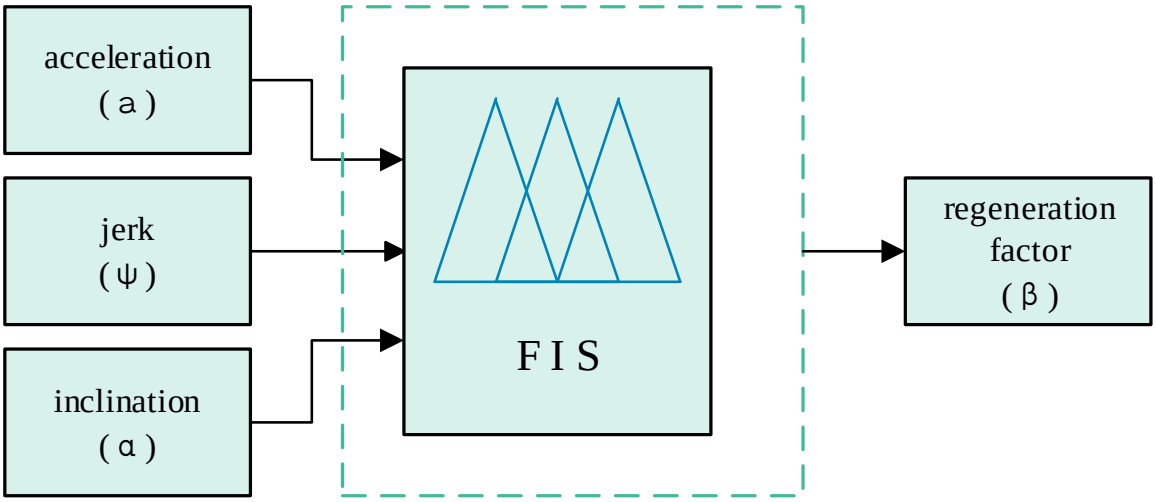

Figure 3. Structure of the fuzzy logic model of regenerative braking factor based on Fuzzy inference system (FIS) (from Maiaa et al. [60]).

Hybrid Model for EV Energy Consumption Rate Estimation

In the proposed hybrid approach, the model variables are carefully selected based on the EV physical model instead of blindly exhausting a long list of variables and their combination. Then, a multi-linear regression (MLR) model is employed to calibrate the corresponding coefficients. The proposed approach excels in real-time performance but is more adaptive to different driving conditions without significantly compromising the model accuracy, when compared to a knowledge-based approach (e.g., [*48*]). The latter may require a large effort to measure the related parameters and calibrate the coefficients for the electric vehicle in a specific condition.

Based on the battery power equations (Eq. (1)-(3)) and the characteristics of regenerative braking systems discussed above, two types of "hybrid" regression models are proposed for EV energy consumption rate estimation. The major difference of these two models lies in the complexity of modeling the regenerative braking effects. For simplicity, we assume the transmission efficiency η_t and motor efficiency η_m as constants.

A Type I hybrid energy consumption model is formulated in Eq. (5), which simply considers the regenerative braking factor as a linear function of the vehicle's speed, or $k \propto v$. Therefore,

$$P_{est} = l_0 + l_1 v cos(\alpha) + l_2 v sin(\alpha) + l_3 v^3 + l_4 va + l_5 v^2 cos(\alpha) + l_6 v^2 sin(\alpha) + l_7 v^4 + l_8 v^2 a \quad (5)$$

For comparison, we also applied the Type I hybrid energy consumption rate model to the subsets of data partitioned according to Eq. (4), i.e., $v < 5\ m/s$ and $v \geq 5\ m/s$, and calibrated the coefficients, respectively. However, further investigation is needed to evaluate the impacts of the speed threshold.

In the Type II model, we considered the regenerative braking factor to be related to not only the vehicle's speed but also the other factors mentioned above, including acceleration, jerk, and road grade. Based on the fuzzy logic model provided by Maiaa et al. [*60*], we estimated the regeneration factor using our field driving data. Further dependency tests showed that jerk (ψ) may not be a significant indicator, so we did not include it in the model. The resulting Type II MLR model is shown in Eq. (6):

$$P_{est} = l_0 + l_1 v cos(\alpha) + l_2 v sin(\alpha) + l_3 v^3 + l_4 va + l_5 v^2 cos(\alpha) + l_6 v^2 sin(\alpha) + l_7 v^4 + l_8 v^2 a + l_9 vacos(\alpha) + l_{10} vasin(\alpha) + l_{11} v^3 a + l_{12} va^2 + l_{13} v\alpha cos(\alpha) + l_{14} v\alpha sin(\alpha) + l_{15} v^3 \alpha + l_{16} va \quad (6)$$

Table 2 and Table 3 list the calibration parameters for the Type I and Type II hybrid energy consumption rate models. In our study, we chose the Type I model to balance model complexity (such as number of variables) with computational efficiency.

Table 2. Parameter calibration results of the Type I hybrid energy consumption rate model.

Variable	Coefficient	p-value
Intercept	-3.146	$< 2 \times 10^{-16}$
$vcos(\alpha)$	-0.940	$< 2 \times 10^{-16}$
$vsin(\alpha)$	-1.237	$< 2 \times 10^{-16}$
v^3	-	-
va	-1.521	$< 2 \times 10^{-16}$
$v^2 cos(\alpha)$	4.104×10^{-2}	$< 2 \times 10^{-16}$
$v^2 sin(\alpha)$	3.289×10^{-2}	5.03×10^{-11}
v^4	-4.427×10^{-5}	$< 2 \times 10^{-16}$
$v^2 a$	-	-
Adjusted R^2	0.677	

Table 3. Parameter calibration results of Type II hybrid energy consumption rate model.

Variable	Coefficient	p-value
Intercept	-3.037	$< 2 \times 10^{-16}$
$vcos(\alpha)$	-0.591	3.32×10^{-16}
$vsin(\alpha)$	-	-
v^3	-1.047×10^{-3}	$< 2 \times 10^{-16}$
va	-1.403	$< 2 \times 10^{-16}$
$v^2cos(\alpha)$	2.831×10^{-2}	1.03×10^{-10}
$v^2sin(\alpha)$	-	-
v^4	-	-
v^2a	-7.980×10^{-2}	1.60×10^{-5}
$vacos(\alpha)$	-	-
$vasin(\alpha)$	-1.490	1.13×10^{-5}
v^3a	3.535×10^{-3}	5.60×10^{-9}
va^2	-0.243	$< 2 \times 10^{-16}$
$va\alpha cos(\alpha)$	-1.279	$< 2 \times 10^{-16}$
$va\alpha sin(\alpha)$	-	-
$v^3\alpha$	6.484×10^{-4}	$< 2 \times 10^{-16}$
$va\alpha$	0.998	4.79×10^{-4}
Adjusted R^2	0.729	

Machine Learning–based Vehicle Speed Forecasting

In this study, we aimed to develop a direct time series forecasting model with a second-by-second vehicle speed trajectory detected by onboard sensors (e.g., radar) as inputs. The historical speed horizon of the input and forecasting horizon of the output are both in three time steps (i.e., 3 seconds) for training and testing the speed forecasting models. We implement a Radial Basis Function Neural Network (RBF-NN) for vehicle speed forecasting and compare its performance with other well-known nonlinear regression models like Gaussian Processes (GP) and Multi-Layer Perceptron Neural Network (MLP-NN) for different driving scenarios. The general RBF-NN based vehicle speed predictor has a feed-forward neural network framework with one hidden layer in which the nodes have radial transfer function, as shown in Figure 4. The network input is a vector containing the vehicle's historical speed trajectory of the preceding 3 seconds, and the output is a predicted speed trajectory within a 3-second horizon.

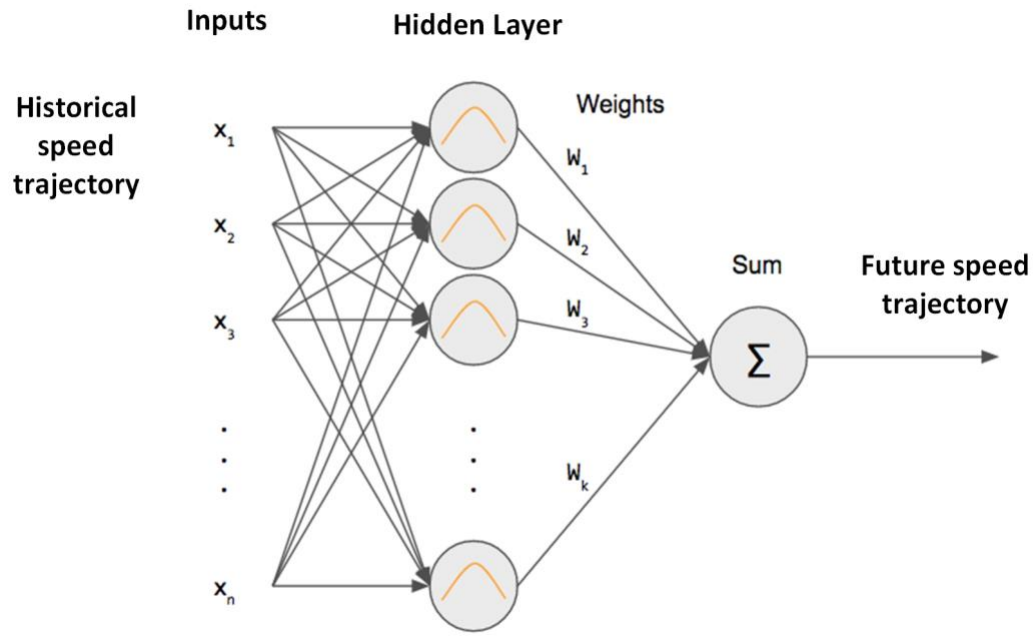

Figure 4. Structure of the radial basis function–based vehicle speed predictor.

The implemented RBF-NN is a three-layer feed-forward network with K hidden nodes. A radial basis function needs to be pre-defined for each hidden node to activate neurons in the hidden layer. Each hidden node contains a nonlinear activation function. Here, we chose the Gaussian function as the activation function for the RBF-NN, formulated as:

$$\varphi_j(x) = exp\left[-\left(\bar{x} - \mu_j\right)^T \Sigma_j^{-1}\left(\bar{x} - \mu_j\right)\right] \quad (7)$$

$$y_k(x) = \sum_{j=1}^{M} w_{kj}\, \varphi_j(x) + b_{kj}, \quad (8)$$

where φ_j is the activated function of node j; $\bar{x}$ is the input vector for node j; w_{kj} is the output weight and b_{kj} is the constant bias; and μ_j and $\sum_j$ are the mean vector and covariance matrix of the j^{th} Gaussian function. The mean μ_j represents the center, and $\sum_j$ indicates the shape of the activation function. Finally, the output of each node at the RBF-NN's output layer is computed as a linear combination of the outputs of the hidden nodes.

An advantage of an RBF-NN compared to a Gaussian Process and MLP-NN is the efficiency of training based on a two-stage procedure. The time complexity of training in a Gaussian Process for prediction increases exponentially with the sample size, which becomes quite an issue when applied to a large network in real time. An MLP-NN could have more than one hidden layer, uses an iterative technique, and works globally, while an RBF-NN has only one hidden layer, is based on a non-iterative technique, and acts as a local approximation. Besides, an RBF-NN is more robust to adversarial noise and easier to generalize than is an MLP-NN. In the first stage of RBF-NN training, the parameters of the basis function are set to model unconditional data density. The centers of our trained RBF network are determined by fitting a Gaussian mixture model with circular covariance, using the Expectation-Maximization (EM) algorithm. The second stage of training determines the weights between the hidden layer and the output layer by using the Moore-Penrose generalized pseudo-inverse, which overcomes many issues in traditional gradient algorithms such as stopping criterion, learning rate, number of epochs, and local minima. The structure of the RBF-NN was optimized by pruning the network based on 5-fold cross validation in this study. We selected an RBF-NN for real-time vehicle speed forecasting in urban driving because of its shorter training time, forecasting accuracy, and generalizability. Figure 5 illustrated an example of forecasted speed trajectory using RBF-NN, where those short segments represent the short term (3 seconds) forecasting results.

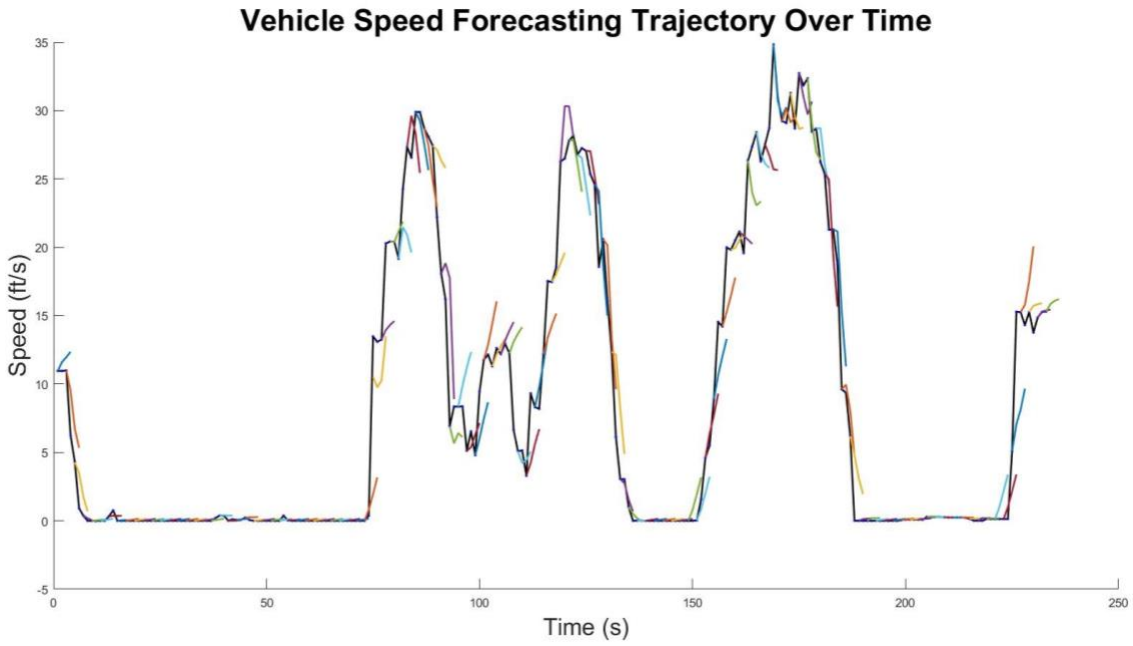

Figure 5. An example of speed trajectory forecasting using RBF-NN.

Deep Learning–based Eco-Approach and Departure

System Architecture

Figure 6 presents the system architecture of the proposed algorithm. As illustrated in the figure, the architecture is divided into two portions: an off-line process (upper portion) and an on-line process (lower portion). In the off-line process, vehicle dynamics (e.g., speed and acceleration) and powertrain operation (e.g., engine/motor speed, engine/motor torque, and gear ratio if any) from real-world testing are first logged via on-board diagnostics (OBD) systems. These data are then post-processed to characterize the specific powertrain model, which is used to build the components of a graph-based trajectory planning algorithm (GTPA) developed in our previous study [*61*]. This GPTA includes nodes (discretized states in the velocity-time-distance space), links (feasible transition from one state to another), and associated link costs (fuel consumption for the state transition at each time step). The *Database from Simulation Runs* module contains possible vehicle dynamics and SPaT values that are expected for the testing scenarios. The GTPA is called for the values in the database to find an associated optimal speed trajectory profile as the target vehicle approaches an intersection. Towards that end, a deep neural network model is trained using the same inputs to the GTPA as training features and the same computed paths used by the GTPA as target values. By parsing the optimal paths, the Deep Learning Trajectory Planning Algorithm (DLTPA) can learn to predict the velocity for the next time step. In other words, DLTPA is developed and trained to approximate the GTPA's optimal performance.

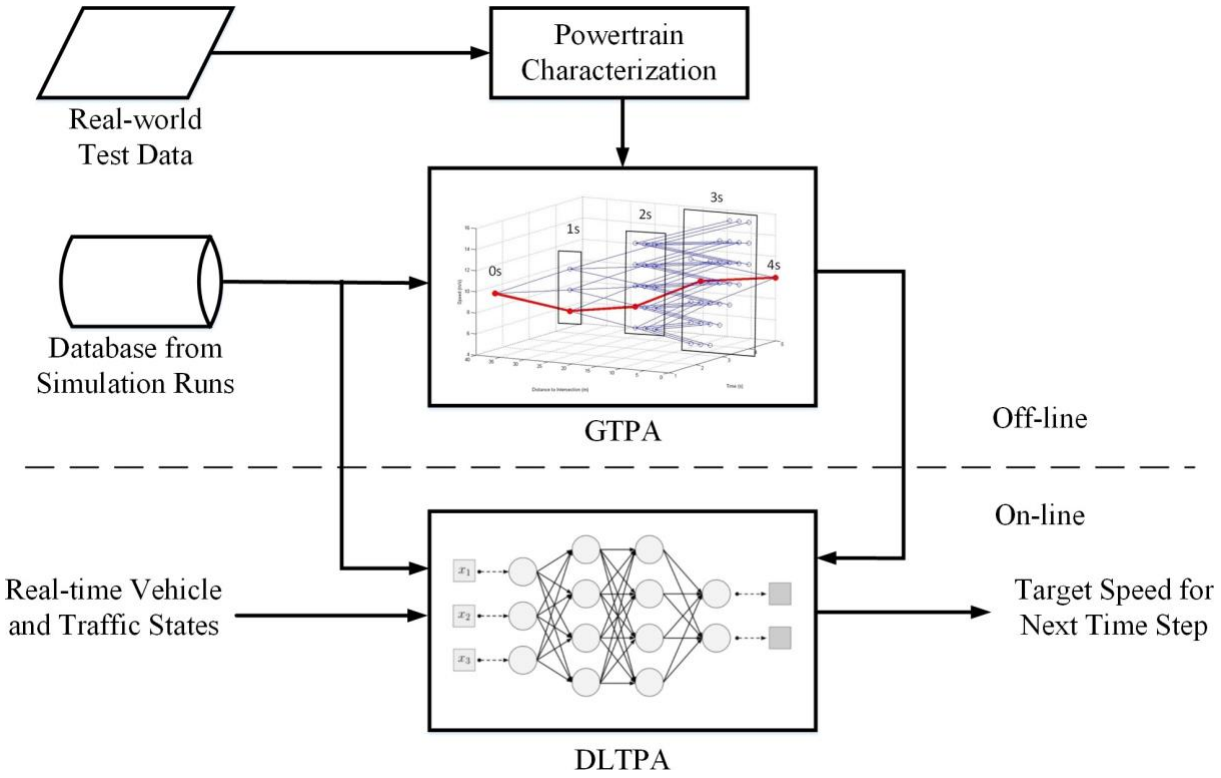

Figure 6. System architecture for deep learning–based EAD.

Once DLTPA is trained off-line, it will be adopted for on-line implementation. In this study, an Application Programming Interface (API) is developed for the DLTPA module in a microscopic traffic simulation environment, where vehicle and traffic states feed into DLTPA in real time and the prediction by DLTPA is used as the target velocity of the host vehicle for the next time step. The details on the creation of the training dataset for DLTPA and construction of the deep neural network are presented in the next section.

DLTPA Description

The DLTPA uses an MLP-NN. This type of neural network takes as input one or more parameters. It is trained on previous inputs and the corresponding expected outputs. After training, it predicts an output when given a new input. An MLP-NN contains a variable number of nodes. Each node performs an activation function on an input, such as rectified linear unit (ReLU), tangent hyperbolic, or linear. The input to the activation function is a weighted sum of all the input parameters to the node. The architecture of a node is shown in Figure 7.

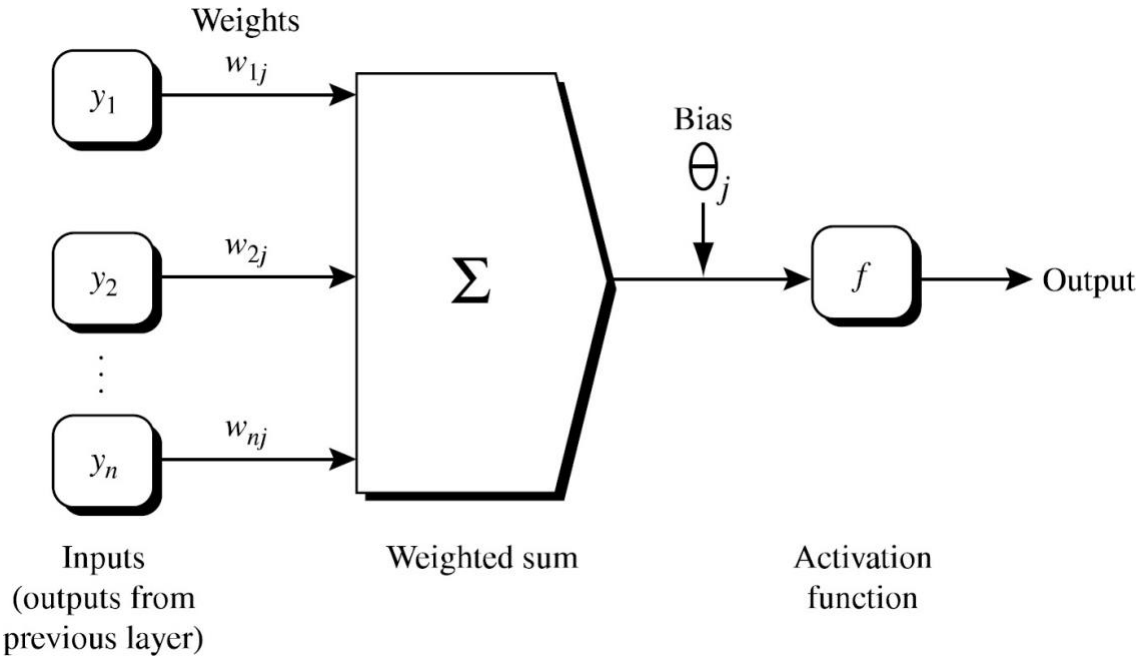

Figure 7. Architecture of an MLP node.

An MLP-NN is made up of 3 types of layers of nodes. The first layer is called the input layer. It is where known parameters initially enter the MLP. In Figure 8, the nodes labeled 1, 2, and 3 make up the input layer, and X1, X2, X3 are the inputs. Following the input layer is one or more hidden layers. The nodes labeled 4, 5 in Figure 8 make up a hidden layer. The hidden layer generally has a non-linear activation function in each node, such as ReLU. The last type of layer is the output layer, which follows the last hidden layer. The output layer formats the output to be consistent with the format of the expected predictions. In Figure 8, the output layer is the node labeled 6.

Each node in a layer is connected by an edge to one or more nodes in the next layer, with the exception of the output layer. A common architecture, and the one that we employed in this study, is to connect all nodes in a layer with every node in the next layer. This is commonly referred to as "densely connected," as shown in Figure 8.

Each edge has an associated weight. The edge weights are the weights used to scale each input to the node when computing the weighted sum. At initialization, the weights are generally random or predefined. During training, the edge weights are adjusted so that the MLP-NN gives better predictions. Training occurs by predicting on a training unit and adjusting the edge weights based on the error between the prediction and the expected value.

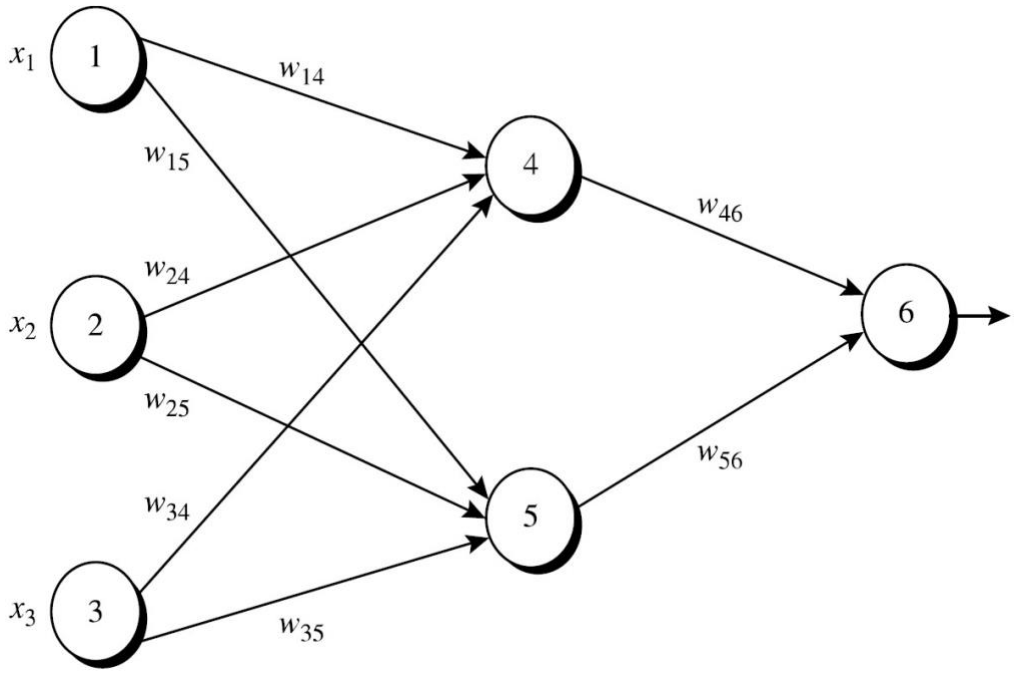

Figure 8. Multilayer perceptron.

The DLTPA uses an MLP-NN known as a regressor. Its architecture follows the architecture described above. Consequently, we choose to use the rectified linear unit (ReLU) for the hidden layer activation functions, whose mathematical formula is given by:

$$f(x) = \begin{cases} 0, & x < 0 \\ x, & x \geq 0 \end{cases}$$

Often a dropout layer is added. This is a simple method that deters the prediction model from memorizing the training data without learning a generalized function. The output layer characterizes the MLP. It is one node with activation $f(x) = x$.

The created dataset is partitioned to determine a neural network architecture. The first partition is a validation training set constituting 60% of all the data. The next 20% is a

validation set. The last 20% is a final test set. Different numbers of hidden layers were run for 300 iterations through the validation training data and compared. Based on this, we chose to use hidden layers with 1024 nodes. The accuracy after each iteration was tested against the validation set and plotted. The results for different neural network architectures are shown in Figure 9. One hidden layer converges quickly but shows little potential for gaining accuracy from increased data. Three hidden layers may create difficulty because they require more iterations through the data, which may cause over-fitting. We chose to use an MLP-NN with 2 hidden layers. We used 250 iterations through the training data because the validation plots showed little improvement after 250 iterations. Our final architecture is provided here.

Dense: nodes = 1024; activation = ReLU; Dropout: rate = 0.50

Dense: nodes = 1024, activation = ReLU; Dropout: rate = 0.50

Dense: nodes = 1, activation = linear

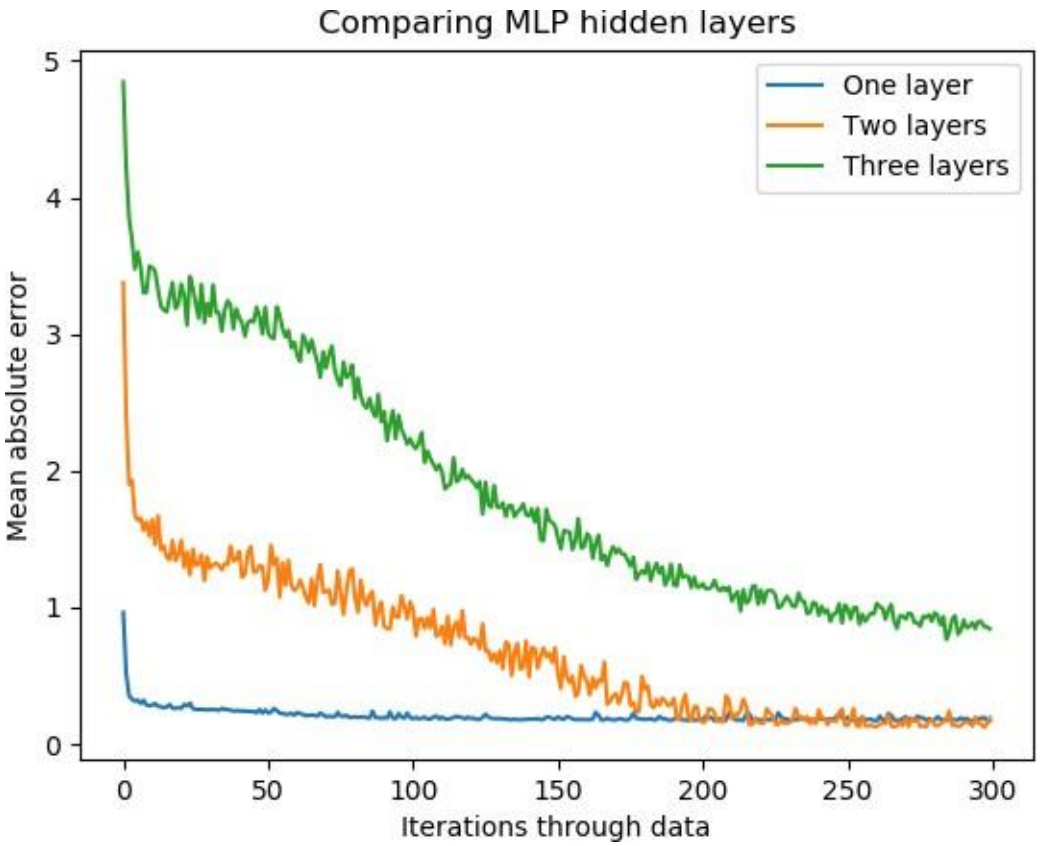

Figure 9. Comparison for one, two, and three hidden layers.

Simulation Study

Setup

We used PTV Vissim (http://vision-traffic.ptvgroup.com/en-us/home/) as our microscopic traffic simulation tool to model the vehicle dynamic and movement on a road network. The simulated network is a 3-mile signalized corridor with 11 signalized intersections along University Ave in Riverside, CA.

Computational Time Comparison

The DLTPA was evaluated against the GTPA in terms of computational time in simulation by controlling one electric vehicle for 10 different simulation seeds. Different seeds have different times at which the controlled vehicle enters simulation. Consequently, this affects the signal phase and timing (SPaT) that the vehicle encounters in the simulation. The results are shown in Table 4. Since the DLTPA is executed at each timestep, the total computational time is amortized over the entire path. On the other hand, the computational time of the GTPA is not evenly distributed, based on our experience. A major portion of the computational time is consumed when generating a path. This advantage makes the DLTPA more applicable to real world scenarios.

Table 4. Computational time comparison in simulation.

Run	GTPA (second)	DLTPA (second)
1	32	11
2	53	11
3	25	11
4	62	11
5	39	11
6	74	11
7	48	11
8	105	11
9	69	11
10	80	11

The computational time of the DLTPA is constant for an intersection despite the vehicle states and SPaT. This feature makes the DLTPA more attractive than the GTPA in real world implementation. Although there is one instance where the computation time is slightly off from the rest of the simulation runs, we attribute this small variation to other disturbances in the simulation runs. When we compare the results between the GTPA and DLTPA, we note that the

mean absolute errors vary from 1.07 to 1.83 across different seeds. Figure 9 illustrates some example trajectory results from the GTPA and DLTPA.

Energy Consumption Results

A single electric vehicle was running along the simulated corridor in traffic for 10 different simulation runs (with different seeds) under different control strategies. For each run, the energy consumption using the VISSIM by-default control (baseline), DLTPA and GTPA were recorded in separate simulations. Results are provided in Table 5. Columns 2-4 show the energy used by each method in kilojoules/meter (kJ/meter). Columns 5-6 show the improvement in percentage of the DLTPA and GTPA compared to the baseline. In some simulation runs, the DLTPA actually performed better than the GTPA. We hypothesize that small prediction errors affect simulation events. For example, a vehicle might enter a queue before the controlled vehicle in the GTPA simulation but not in the DLTPA simulation because the controlled vehicle in the DLTPA simulation was moving slightly faster than the controlled vehicle in the GTPA simulation. On average, the DLTPA uses 0.006 kJ/meter more energy than the GTPA and provides 0.61% less improvement to the baseline energy consumption than the GTPA. Nevertheless, the DLTPA outperforms the baseline scenarios by 13.76%. Figure 10 gives an example of speed trajectories based on DLTPA vs. GTPA.

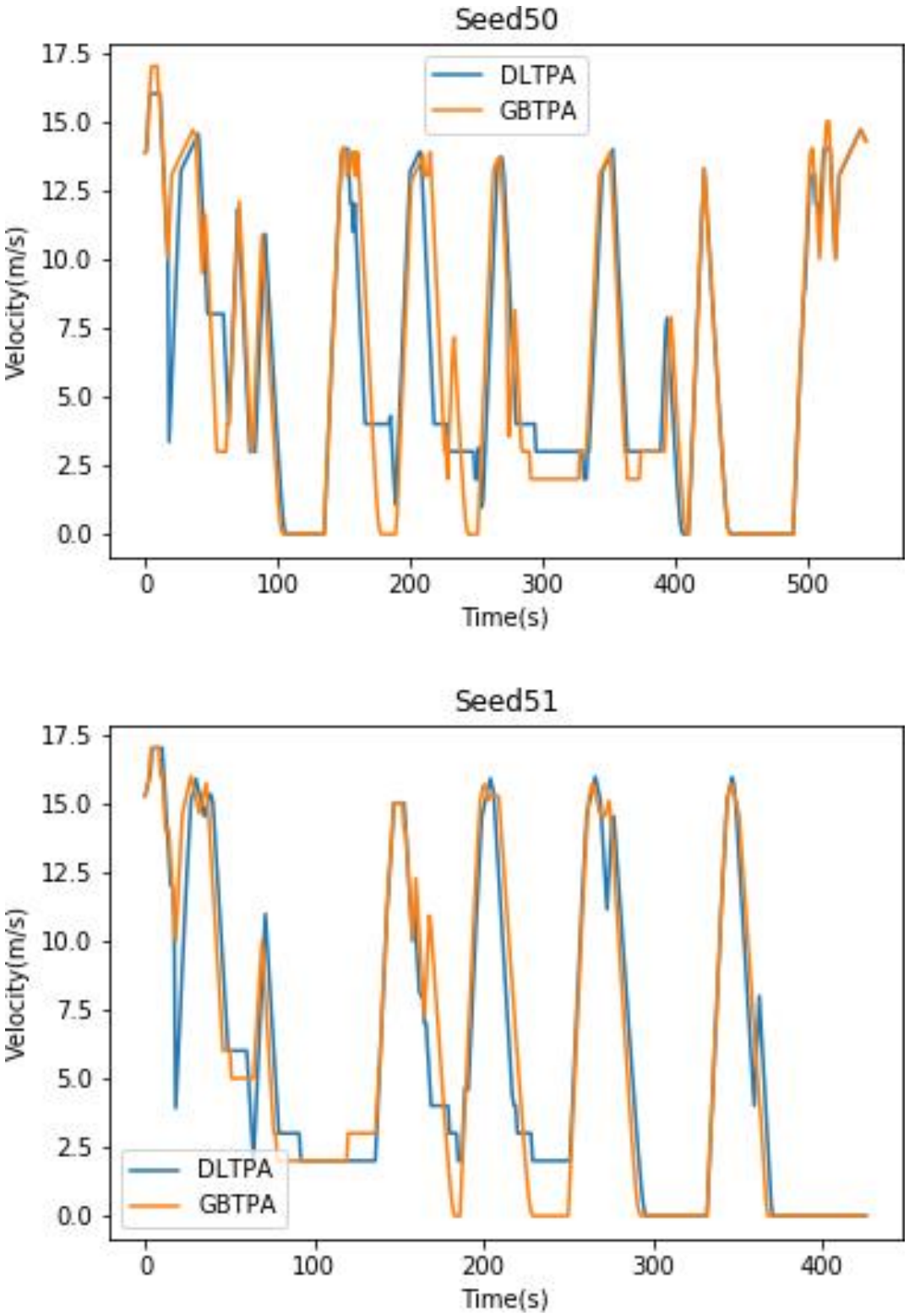

Figure 10. Example trajectories of GTPA vs. DLTPA.

Table 5. Comparative results of energy consumption.

Run	Absolute Energy Consumption (kJ/m)			% Improvement	
	Baseline	DLTPA	GTPA	DLTPA	GTPA
1	0.650	0.569	0.613	12.46	5.69
2	0.699	0.610	0.522	12.73	25.32
3	0.668	0.596	0.594	10.78	11.08
4	0.738	0.618	0.590	16.26	20.05
5	0.677	0.577	0.619	14.77	8.57
6	0.729	0.609	0.605	16.46	17.01
7	0.680	0.600	0.620	11.76	8.82
8	0.740	0.585	0.537	20.95	27.43
9	0.638	0.591	0.639	7.37	-0.16
10	0.725	0.623	0.581	14.07	19.86
Avg.	0.694	0.598	0.592	13.76	14.37
SD	0.037	0.018	0.037	3.69	8.95

Conclusion

The proposed DLTPA can significantly reduce the computational time to constant complexity (O(1)). Further, it addresses the issue of inflexibility to rapidly changing traffic conditions by predicting only the velocity for the next timestep. We tested this innovative Eco-Approach and Departure (EAD) algorithm against the GTPA (which was also developed in our previous work) in a simulation environment. In summary,

- This project developed an innovative deep learning–based Eco-Approach and Departure algorithm for electric vehicles with customized powertrain models.
- The proposed DLTPA can significantly reduce the computational complexity of the trajectory planning algorithm, which is favorable for real-time implementation.
- The proposed DLTPA can increase the flexibility of the trajectory planning algorithm in response to a rapidly changing environment.
- Based on the preliminary simulation study in VISSIM, the DLTPA can provide a 13.76% improvement above the baseline. The results from the DLTPA consume only 0.006 kJ/meter more energy per distance than the GTPA (which is considered to be an optimal solution in terms of energy efficiency) but significantly improve the computational efficiency by up to 90% (e.g., simulation run #8 in Table 4).

References

1. Bureau of Transportation Statistics (BTS). *Transportation Statistics Annual Report (TSAR) 2017*, Chapter 7, May 2018
2. U.S. Environmental Protection Agency (USEPA). *Inventory of U.S. Greenhouse Gas Emissions and Sinks: 1990 - 2016*, Final Report EPA 430-R-18-003, April 2018.
3. U.S. Department of Transportation. *Applications for the Environment: Real-Time Information Synthesis*. https://www.its.dot.gov/research_archives/aeris/index.htm. Accessed on December 15th, 2018.
4. European Commission (EC). *eCoMove – Cooperative Mobility Systems and Services for Energy Efficiency*. http://www.ecomove-project.eu/. Accessed on December 15th, 2018.
5. US Department of Transportation. *Connected Vehicle Reference Implementation Architecture (CVRIA) Version 3*, https://www.its.dot.gov/research_archives/arch/cvria2.htm. Accessed on January 15th, 2019.
6. U.S. Department of Transportation. *Environment – Eco Approach and Departure at Signalized Intersections*. https://www.its.dot.gov/infographs/Eco_approach_departure.htm. Accessed on July 15th, 2018.
7. Li, M., K. Boriboonsomsin, G. Wu, W. Zhang, and M. Barth. Traffic Energy and Emission Reductions at Signalized Intersections: A Study of the Benefits of Advanced Driver Information. *International Journal of ITS Research*, 2009.
8. Wu, G., K. Boriboonsomsin, W-B Zhang, M. Li and M. Barth. Energy and Emission Benefit Comparison between Stationary and In-vehicle Advanced Driving Alert Systems. *Transportation Research Record: Journal of the Transportation Research Board*. No. 2189, 2010, pp. 98–106.
9. Katsaros, K., R. Kernchen, M. Dianati, and D. Rieck. *Performance Study of a Green Light Optimized Speed Advisory (GLOSA) Application using an Integrated Cooperative ITS Simulation Platform*. The 7th International Wireless Communications and Mobile Computing Conference, Istanbul, Turkey, July 2011.
10. Garcia-Castro, A., A. Monzon, C. Valdes and M. Romana. Modeling Different Penetration Rates of Eco-Driving in Urban Areas: Impacts on Traffic Flow and Emissions. *International Journal of Sustainable Transportation*, Vol. 11, No. 4, 2017, pp. 282–294.
11. Mandava, S., K. Boriboonsomsin and M. Barth. Arterial Velocity Planning based on Traffic Signal Information under Light Traffic Conditions. The 12th International IEEE Conference on Intelligent Transportation Systems, St. Louis, MO, October 2009.
12. Kamal, M.A.S., M. Mukai, J. Murata and T. Kawabe. Ecological Driver Assistance System Using Model Based Anticipation of Vehicle-Road-Traffic Information. *IET Journal of Intelligent Transportation Systems*, 4 (4), 2010, pp. 244–251.
13. Rakha, H., and R. Kamalanathsharma. Eco-driving at Signalized Intersections Using V2I Communication. The 14th IEEE Conference on Intelligent Transportation Systems (ITSC), Washington, D.C., USA. October 2011.

14. Asadi, B. and A. Vahidi. Predictive Cruise Control: Utilizing Upcoming Traffic Signal Information for Improving Fuel Economy and Reducing Trip Time. *IEEE Transactions on Control Systems Technology*, 19 (3), 2011, pp 707–714.
15. Katsaros, K., R. Kernchen, M. Dianati, D. Rieck, and C. Zinoviou. Application of Vehicular Communications for Improving the Efficiency of Traffic in Urban Areas. *Wireless Communications and Mobile Computing*, Vol. 11, 2011, pp. 1657–1667.
16. Chen, Z., Y. Zhang, J. Lv, and Y. Zou. Model for Optimization of Eco-driving at Signalized Intersections. *Transportation Research Record*, No. 2427, 2014, pp. 54–62.
17. Jin, Q., G. Wu, K. Boriboonsomsin, and M. Barth. Power-Based Optimal Longitudinal Control for a Connected Eco-Driving System. *IEEE Transactions on Intelligent Transportation Systems*, 17 (10), 2016, pp. 2900–2910.
18. Li, S., S. Xu, X. Huang, B. Cheng, and H. Peng. Eco-Departure of Connected Vehicles with V2X Communication at Signalized Intersections. *IEEE Transactions on Vehicular Technology*, 64 (12), 2015, pp. 5439–5449.
19. Huang, X., and H. Peng. Speed Trajectory Planning at Signalized Intersections with Sequential Convex Optimization. Proceedings of the 2017 American Control Conference, Seattle, WA, USA, 2017.
20. Huang, K., X. Yang, Y. Lu, C. Mi, P. Kondlapudi. Ecological Driving System for Connected/Automated Vehicles Using a Two-Stage Control Hierarchy. *IEEE Transactions on Intelligent Transportation Systems*, 19 (7), 2018, pp. 2373–2384.
21. Xia, H., K. Boriboonsomsin, and M. Barth. Dynamic Eco-Driving for Signalized Arterial Corridors and Its Indirect Network-Wide Energy/Emissions Benefits. *Journal of Intelligent Transportation Systems*, Vol. 17, 2013, pp. 31–41.
22. Xia, H., K. Boriboonsomsin, F. Schweizer, A. Winckler, K. Zhou, W-B. Zhang, and M. Barth. Field Operational Testing of ECO-Approach Technology at a Fixed-Time Signalized Intersection. The 15th IEEE Intelligent Transportation Systems Conference, Anchorage, AK, September 2012.
23. Wu, G., K. Boriboonsomsin, H. Xia, and M. Barth. Supplementary Benefits from Partial Vehicle Automation in an Eco-Approach and Departure Application at Signalized Intersections. *Transportation Research Record: Journal of the Transportation Research Board*, Vol. 2424, 2014, pp. 66–75.
24. Altan, O., G. Wu, M. Barth, K. Boriboonsomsin and J. Stark. GlidePath: Eco-Friendly Automated Approach and Departure at Signalized Intersections. *IEEE Transactions on Intelligent Vehicles*, 2 (4), 2017, pp. 266–277.
25. Kamalanathsharma, R. and H. Rakha. Multi-Stage Dynamic Programming Algorithm for Eco-speed Control at Traffic Signalized Intersections. The 16th International IEEE Conference on Intelligent Transportation Systems, the Hague, Netherlands, October 2013.
26. Wan, N., A. Vahidi, and A. Luckow. Optimal Speed Advisory for Connected Vehicles in Arterial Roads and the Impact on Mixed Traffic. *Transportation Research Part C: Emerging Technology*, Vol. 69, 2016, pp. 548–563.

27. Jiang, H., J. Hu, S. An, M. Wang, and B. Park. Eco Approaching at an Isolated Signalized Intersection under Partially Connected and Automated Vehicles Environment. *Transportation Research Part C: Emerging Technology*, Vol. 79, 2017, pp 290–307.
28. He, X., H. Liu, X. Liu. Optimal Vehicle Speed Trajectory on a Signalized Arterial with Consideration of Queue. *Transportation Research Part C: Emerging Technology*, Vol. 61, pp. 106-120, Dec. 2015.
29. Ye, F., P. Hao, X. Qi, G. Wu, K. Boriboonsomsin, and M. Barth. Prediction-based Eco-Approach and Departure at Signalized Intersections with Speed Forecasting on Preceding Vehicles. *IEEE Transactions on Intelligent Transportation Systems*, 2018.
30. Mahler, G., and A. Vahidi. An Optimal Velocity-Planning Scheme for Vehicle Energy Efficiency through Probabilistic Prediction of Traffic-Signal Timing. *IEEE Transactions on Intelligent Transportation Systems*, Vol. 15, 2014, pp. 2516–2523.
31. P. Hao, G. Wu, K. Boriboonsomsin, M. Barth. Eco-Approach and Departure (EAD) Application for Actuated Signals in Real-World Traffic. *IEEE Transactions on Intelligent Transportation Systems*, 2018.
32. Sun, C., X. Shen, and S. Moura. Robust Optimal Eco-driving Control with Uncertain Traffic Signal Timing. American Control Conference, 2018.
33. Wu, G., P. Hao, Z. Wang, K. Boriboonsomsin, and M. Barth. Eco-Approach and Departure along Signalized Corridors. Presented at 98th Annual Meeting of the Transportation Research Board, Washington, D.C., 2019.
34. Yang, S. C., M. Li, Y. Lin, and T. Q. Tang. Electric Vehicle's Electricity Consumption on a Road with Different Slope. *Phys. A,* Vol 402, pp. 41-48, 2014.
35. Zhang, R. and E. Yao. Eco-driving at Signalized Intersections for Electric Vehicles. *IET Intelligent Transport Systems*, Vol 9, pp. 488-497, June 2015.
36. Baouche, F., E. L. Trigui, N. E. Faouzi, and R. Billot. Energy Consumption Assessment for Electric Vehicles. International Symposium on Recent Advances in Transport Modeling, p.5, 2013.
37. Alvarex, D., F. S. Garcia, J. E. Naranjo, J. J. Anaya, and F. Jimenez. Modeling the Driving Behavior of Electric Vehicles Using Smartphones and Neural Networks. *Intel. Transp. Syst. Magazine*, Vol 6, pp. 44-53, 2014.
38. Chang, N., D. Baek, and J.Hong. Power Consumption Characterization, Modeling and Estimation of Electric Vehicles. IEEE/ACM International Conference on Computer Aided Design (ICCAD), pp. 175-182, 2014.
39. Yao, E., M. Wang, Y. Song, and Y. Zhang. Estimating Energy Consumption based on Microscopic Driving Parameters for Electric Vehicles. Presented in Transportation Research Board 93rd Annual Meeting, 2014.
40. Wu, X., D. Freese, A. Cabrera, and W. A. Kitch. Electric Vehicles' Energy Consumption Measurement and Estimation. *Transportation Research Part D: Transport and Environment*, vol. 34, Pages 52-67, January 2015.

41. Ehsani, M., Y. Gao, and A. Emadi. Modern Electric, Hybrid Electric, and Fuel Cell Vehicles: Fundamentals, Theory, and Design. Power Electronics and Applications Series (2nd). CRC press, 2010.
42. Felipe, J., J. C. Amarillo, J. E. Naranjo, F. Serradilla and A. Díaz. Energy Consumption Estimation in Electric Vehicles Considering Driving Style. 2015 IEEE 18th International Conference on Intelligent Transportation Systems, Las Palmas, pp. pp. 101-106, 2015.
43. Schubert, R., E. Richter, and G. Wanielik. Comparison and Evaluation of Advanced Motion Models for Vehicle Tracking. International Conference on Information Fusion, Cologne, Germany, Jul. 2008.
44. Lefevre, S., C. Sun, R. Bajcsy, C. Laugier. Comparison of Parametric and Non-parametric Approaches for Vehicle Speed Prediction. In Proc. Amer. Control Conf. (ACC), pp. 3494–3499, June 2014.
45. Elhenawy, M. and H. Rakha. Traffic Stream Speed Short-term Prediction Using Machine Learning: I-66 Case Study. In Transportation Research Board 95th Annual Meeting. No. 16-3805, 2016.
46. Houenou, A., P. Bonnifait, V. Cherfaoui, and Y. Wen. Vehicle Trajectory Prediction based on Motion Model and Maneuver Recognition. Japan, IEEE-IROS, 2013.
47. Wiest, J., M. Hoffken, U. Kresel, and K. Dietmayer. Probabilistic Trajectory Prediction with Gaussian Mixture Models. In Proc. IEEE IV Symp., pp. 141–146, June 2012.
48. Jungme, P., L. Dai, Y. L. Murphey, J. Kristinsson, R. McGee, K. Ming, and T. Phillips. Intelligent Speed Profile Prediction on Urban Traffic Networks with Machine Learning. In Proc. Int. Joint Conf. Neural Netw., pp. 2991–2996, 2011.
49. Jiang, B. and Y. Fei. Traffic and Vehicle Speed Prediction with Neural Network and Hidden Markov Model in Vehicular Networks. In Intelligent Vehicles Symposium (IV), 2015 IEEE, pp. 1082–1087, IEEE, 2015.
50. Jiang, B. and Y. Fei. Vehicle Speed Prediction by Two-Level Data Driven Models in Vehicular Networks. *IEEE Trans. Intelligent Transportation Systems*, Vol. 18, No. 7, pp. 1793-1801, July 2017.
51. Wang, et al. TrackT: Accurate Tracking of RFID Tags with mm-Level Accuracy Using First-Order Taylor Series Approximation. *Ad Hoc Netw.*, Vol. 53, pp. 132–144, December 2016.
52. Wang, Z., N. Ye, R. Malekian, R. Wang, and P. Li. TMicroscope: Behavior Perception Based on the Slightest RFID Tag Motion. *Elektronika Electrotechnika*, Vol. 22, No. 2, pp. 114–122, 2016.
53. Song, X., H. Kanasugi, and R. Shibasaki. Deeptransport: Prediction and Simulation of Human Mobility and Transportation Mode at a Citywide Level. In *IJCAI*, Vol. 16, 2016, pp. 2618–2624.
54. Dabiri, S. and K. Heaslip. Inferring Transportation Modes from GPS Trajectories using a Convolutional Neural Network. *Transportation Research Part C: Emerging Technologies*, Vol. 86, pp. 360–371, 2018.

55. Lv, Y., Y. Duan, W. Kang, Z. Li, F.-Y. Wang et al. Traffic Flow Prediction with Big Data: A deep Learning Approach. *IEEE Trans. Intelligent Transportation Systems*, Vol. 16, no. 2, pp. 865–873, 2015.
56. N. G. Polson, N. G. and V. O. Sokolov. Deep Learning for Short-Term Traffic Flow Prediction. *Transportation Research Part C: Emerging Technologies*, Vol. 79, pp. 1–17, 2017.
57. Belletti, F., D. Haziza, G. Gomes, and A. M. Bayen. Expert Level Control of Ramp Metering based on Multi-task Deep Reinforcement Learning. *IEEE Transactions on Intelligent Transportation Systems*, Vol. 19, no. 4, pp. 1198–1207, 2018.
58. Ma, X., Z. Dai, Z. He, J. Ma, Y. Wang, and Y. Wang. Learning Traffic as Images: a Deep Convolutional Neural Network for Large-scale Transportation Network Speed Prediction. *Sensors*, Vol. 17, no. 4, p. 818, 2017.
59. Huval, B., T. Wang, S. Tandon, J. Kiske, W. Song, J. Pazhayampallil, M. Andriluka, P. Rajpurkar, T. Migimatsu, R. Cheng-Yue et al. An Empirical Evaluation of Deep Learning on Highway Driving. arXiv preprint arXiv:1504.01716, 2015.
60. Maiaa, R., M. Silva, R. Araújoa, and U. Nunes. Electrical Vehicle Modeling: A Fuzzy Logic Model for Regenerative Braking. *Expert Syst. Appl.*, Vol. 42 (1), pp. 8504–8519, Dec. 2015.
61. Hao, P., G. Wu, K. Boriboonsomsin, and M. J. Barth. Eco-approach and Departure (EAD) Application for Actuated Signals in Real-world Traffic. *IEEE Transactions on Intelligent Transportation Systems*, 2018.

Data Management

Products of Research

In this project, we collected detailed data on vehicle dynamics (e.g., speed) and the energy storage system (such as instantaneous current and voltage from the battery pack), and GPS data (for the estimation of road grade) from the test electric vehicle traveling in real-world traffic. These data were used to develop a microscopic energy consumption model for an EV.

Data Format and Content

The data (after processing) were in .csv files. There are two major data sources as specified in the report: one is GPS data, including time stamp (UTC time), latitude, longitude, etc.; the other is CONSULT III+ kit, which monitors the vehicle dynamics (e.g., wheel speed), powertrain operation (e.g., motor speed), and energy flows (e.g., electric current, voltage).

Data Access and Sharing

The data are publicly available via the UC Riverside instance of Dash: https://dash.ucr.edu/stash/, which is in compliance with the USDOT Public Access Plan. The DOI for the dataset is https://doi.org/10.6086/D1FW9G.

Reuse and Redistribution

The data are restricted to research use only. If the data are used, our work should be properly cited: Wu, Guoyuan et al. (2019), Deep Learning–based Eco-driving System for Battery Electric Vehicles, UC Riverside Dash, Dataset, https://doi.org/10.6086/D1FW9G.